Chapter 14
Identifying Priority Areas for Conservation in Mojo River Watershed of Ethiopia Using GIS-Based Erosion Risk Evaluation

Kiflu Gudeta, Mekuria Argaw, and Mengistie Kindu

Abstract Identification of priority areas for the establishment of conservation measures is the first step in conservation planning. Resources may constrain launching of watershed management activities all over a watershed at the same time, hence methods to prioritize intervention are essential. Intensity of land degradation may be one of the key factors to consider in the process of prioritization. This study investigated prioritization of Micro-watersheds (MWs) using soil erosion risk and tested using Mojo River watershed as a case study area. The Revised Universal Soil Loss Equation (RUSLE) and Multi-Criteria Evaluation (MCE) approaches were integrated in GIS environment using remotely sensed and other ancillary data. The analysis showed that RUSLE and MCE help to categorize landscape units into different levels of erosion risk and identify areas that require priority for conservation measures. Based on the RUSLE, MW-level average annual soil loss could be estimated, severity level assessed, and the area covered under various severity levels estimated to support planning. Based on the approach, MW-wise Composite Erosion Index (CEI) could be estimated. As a result, the critical MWs under very high and severe categories were recommended for immediate conservation intervention to reduce on-site and off-site soil loss effects.

K. Gudeta (✉)
Ministry of Agriculture, Addis Ababa, Ethiopia

M. Argaw
Center for Environmental Science, College of Natural and Computational Sciences, Addis Ababa University, Addis Ababa, Ethiopia

M. Kindu
TUM School of Life Sciences Weihenstephan, Institute of Forest Management, Technical University of Munich, Hans-Carl-von-Carlowitz-Platz 2, 85354 Freising, Germany
e-mail: mengistie@tum.de

14.1 Introduction

Soil erosion is the most widespread and multifaceted global land degradation process which leads to a decline in ecosystem services and functions (Adimassu et al. 2014; Haregeweyn et al. 2015). Its on-site and off-site effects threaten food security and economic growth (Hurni 1993; Sutcliff 1993; Tamene 2005; FAO 2019).

In Ethiopia, several studies investigated historical land use land cover (LULC) changes (Bewket 2002; Kindu et al. 2013; Temesgen et al. 2013; Demissie et al. 2017; Gashaw et al. 2018). These studies revealed a worrying trend of LULC changes with consequent soil erosion and land degradation (Tegene 2002; Desalegn et al. 2014; Kindu et al. 2018). The recorded annual soil erosion in Ethiopia ranges from 16 to 300 t/ha/year (Hawando 1995) depending mainly on slope, land cover, and rainfall intensity.

As a consequence of soil degradation, the productive capacity of soils in the Ethiopian highlands has been declining at a rate of 2–3% annually (Hurni 1993). Apart from the adverse effects on land productivity, soil erosion also causes off-site effect and adversely affects irrigation and hydropower generation capacity through sedimentation (Haregeweyn et al. 2015). For instance, sedimentation in Koka hydropower dam of Ethiopia caused potential storage capacity loss. According to EEPC (2002), the rate of siltation in the reservoir had grown from 857 tons/km^2 in 1970 to 2115 tons/km^2/yr. This situation has lowered water volume from the designed live storage capacity of 1667 M m^3 in 1959 to 1186 M m^3 in 1998, which is a loss of 30% of the total storage volume of the reservoir. (EEPC 2002; Elias 2003).

In order to prevent further degradation of upper catchments and to address its off-site effects in lower catchment, information on the extent and spatial distribution of erosion source areas is of paramount importance (Deore 2005; Shi et al. 2003; Tripathi et al. 2003). Because of differences in environmental attributes across landscapes, often few areas of the watershed are responsible to instigate erosion and soil losses. Moreover, limited financial resources often exclude the application of conservation measures all over affected areas at the same time (Tamene 2007; Tripathi et al. 2003). Identification of hot-spot areas of erosion and prioritizing intervention is important to effectively deal with erosion related problems (Khan et al. 2001; Tamene 2005; Kindu et al. 2015).

Various erosion models and/or multi-criteria evaluation approaches integrated with Remote Sensing and GIS have been successfully used in various studies (Tripathi et al. 2003; Deore 2005; Tamene 2007; Asis et al. 2008; Shi et al. 2003; Gashaw et al. 2018; Kindu et al. 2016, 2018; Yahya et al. 2013). This study investigates application of Revised Universal Soil loss Equation (RUSLE) model and multi-criteria evaluation (MCE) approaches integrated with GIS in identifying priority areas for soil erosion conservation using Mojo River Watershed as a case study area. To achieve the research objective, climatological, pedological, topographic, anthropogenic (ground cover) parameters and potential location for gully formation (Tamene 2007) were utilized in the analysis.

14.2   Materials and Methods

14.2.1   Study Area

Mojo River Watershed is located in the main Ethiopian Rift Valley extending up to the eastern escarpment. It is part of the upper Awash River basin in the Eastern Showa Zone of Oromia regional state. Geographically the study area lies between $38°54'\ 10''$ to $39°\ 17'\ 30''$ E and $8°\ 24'\ 57''$ to $9°\ 5'\ 47''$ N. The watershed covers an area of 1680.41 km^2. Elevations of the watershed vary from 1591 to 3069 m asl. Topography of the study area is generally characterized by gently undulating terrain. Of the total area, 61% (1024 km^2) lies within the slope range of 2–10% which is gently flat to undulating topography. Thirty three years (1986–2018) rainfall records for 6 stations within and adjacent to the study area show an average annual rainfall between 772.73 mm and 990.49 mm. The annual temperature of the study area is 19.5 °C with average winter high temperature of 24.1 °C in May and an average low temperature of 14.8 °C in December. Lack of vegetation cover associated with other erosion factors are exposing the area to high rates of soil erosion and loss of soil fertility which inducing heavy silt loads in rivers (Elias 2003).

Secondary data used in location map (Fig. 14.1) gathered from various organizations: towns and administrative boundary from Central Statistics Agency (CSA) (2007); road network from Ethiopian Road Authority (2007); river basin, lakes and soil types (Table 14.1) from Ministry of Water Resources (MoWR) (1999). River network and Mojo River Watershed boundary generated from Digital Elevation Model (DEM) using ArcSWAT.

14.2.2   Data and Preprocessing

In this study, cloud free Landsat OLI imagery acquired on February 1, 2019 (Path/Row is 168/54) was used for mapping land cover and estimating RUSLE *C*-factor. The digital numbers (DN) of the imagery were first converted to at-sensor radiance by using the radiometric calibration parameters in ENVI software. The Fast Line-of-sight Atmospheric Analysis of Spectral Hypercubes (FLAASH) algorithm was then used to convert radiance to reflectance and perform atmospheric correction. Climatic data such as annual rainfall (1986–2018) were gathered from National Meteorological Agency. In addition, a digital elevation model (DEM) with a spatial resolution of 30 m was downloaded from the United States Geological Survey's (USGS) Earth Explorer website (http://earthexplorer.usgs.gov/) for deriving various topographic indices. Field work was carried out during dry season in February 2019 to collect information about vegetation and erosion features in the watershed.
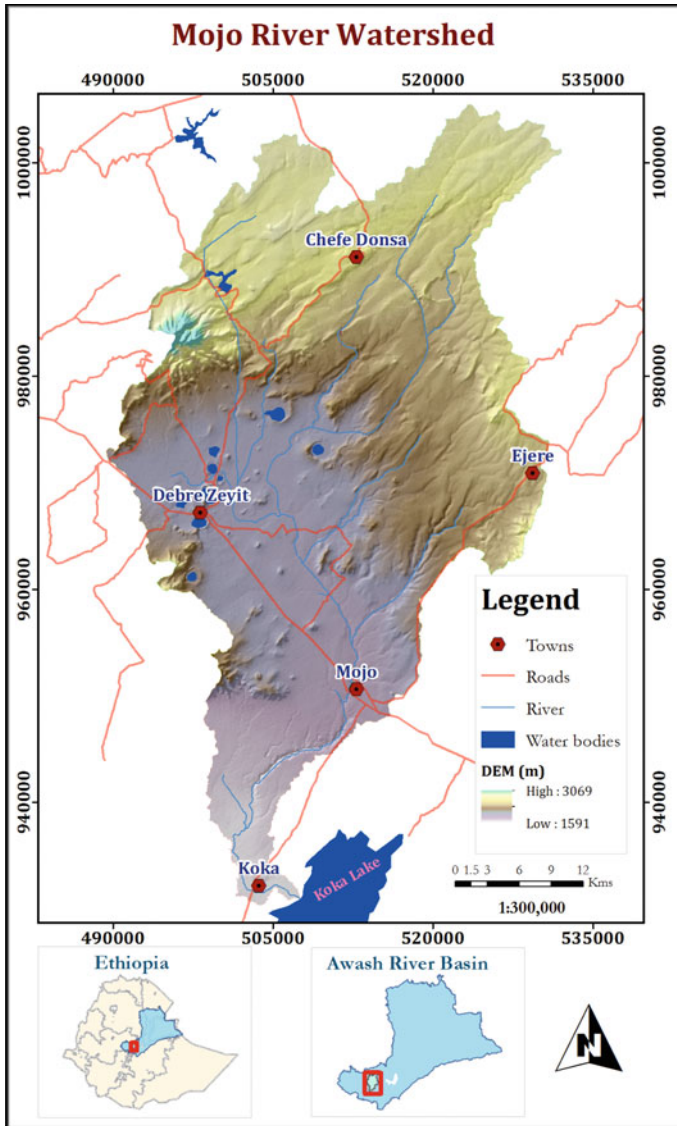
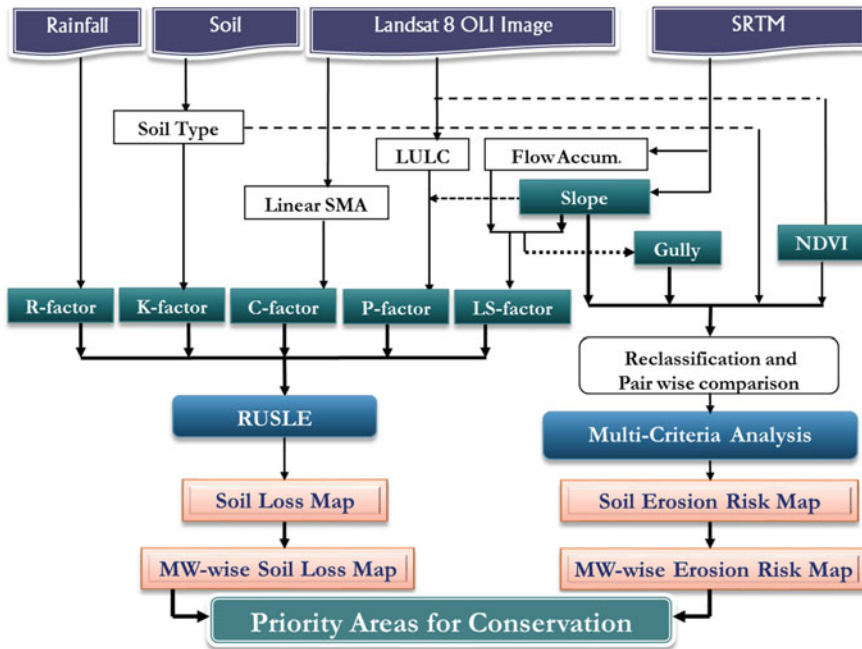**Fig. 14.1** Location map of the study area

Fig. 14.2 Flow chart of research methodology

14.2.3   *Methods of Data Integration and Analysis*

14.2.3.1   **Micro-watershed Delineation for Identifying Priority Areas**

From the 30 m resolution DEM data, Mojo River Watershed and 22 micro-watersheds were delineated using ArcSWAT software. In this study, two approaches were adopted for identifying priority areas in the watershed based on soil erosion-proneness of micro-watersheds. RUSLE was used for estimating soil loss (Renard et al. 1997; FAO 2019; Yahya et al. 2013; Shi et al. 2003) and MCE approach was utilized for mapping erosion risk (Deore 2005; Tamene 2007). The overall methodology is illustrated in Fig. 14.2.

14.2.3.2   **Erosion Factors Generation**

Rainfall Erosivity (*R*) Factor

Potential ability of rain to cause erosion is known as erosivity (*R*-factor). It is defined as the product of kinetic energy and the maximum 30 min intensity and shows the

Table 14.1 Soil types and calculated erodibility factor value

Soil type	Area (km^2)	Percentage	K factor value
Euthric Vertisols	729.12	43.39	0.1440
Vertic Cambisols	674.54	40.14	0.1522
Luvic Phaeozems	138.59	8.25	0.1629
Chromic Luvisols	72.77	4.33	0.1568
Lithic Leptisols	20.41	1.21	0.1632
Haplic Luvisols	18.32	1.09	0.1659
Euthric Fluvisols	14.31	0.85	0.1702
Mollic Andosols	10.57	0.63	0.1660

erosivity of rainfall events (Wischmeier and Smith 1978). Due to rainfall characteristics and absence of automatic hourly rain intensity records in many rainfall stations in Ethiopia, however, it is difficult to apply erosivity equation proposed by Renard et al. (1997) for Ethiopia condition (Nyssen 2001). Therefore, the erosivity factor R was calculated according to the equation given by Hurni (1985), derived from spatial regression analysis (Hellden 1987) for Ethiopian conditions based on easily available mean annual rainfall (P). The R-factor is given by a regression Eq. (14.1):

$$R = -8.12 + 0.562P \tag{14.1}$$

To determine the value of the R-factor, the average of 33-years annual historic rainfall event (1986–2018) was collected from six meteorological stations located within and near the study area. Spline interpolation was done to generate an estimated surface from these scattered sets of point data.

Soil Erodibility (K) Factor

Vulnerability of the soils to get eroded is referred to as erodibility of soils. The K-factor is defined as the rate of soil loss per unit of R-factor on a unit plot (Renard et al. 1997). For Ethiopian condition, Hellden (1987) proposed the K values of the soil based on their color by adapting different sources. Using Eqs. 14.2–14.6 below, the K factor value was estimated for eight soil types identified in the study area (Table 14.1) based on a formula adapted from Yahya et al. (2013) using the FAO harmonized digital soil data.

$$K_{\text{USLE}} = f_{\text{csand}} \cdot f_{\text{cl-si}} \cdot f_{\text{orgC}} \cdot f_{\text{hisand}} \tag{14.2}$$

$$f_{\text{csand}} = \left(0.2 + 0.3 \cdot \text{Exp}\left[-0.256 \cdot m_{\text{s}} \cdot \left(1 + \frac{m_{\text{silt}}}{100}\right)\right]\right) \tag{14.3}$$

$$\text{cl-si} = \left(\frac{m_{\text{silt}}}{m_c + m_{\text{silt}}} \right)^{0.3} \tag{14.4}$$

$$f_{\text{orgC}} = \left(1 - \frac{0.256.\text{orgC}}{\text{orgC} + \text{Exp}[3.72 - 2.95.\ \text{orgC}]} \right) \tag{14.5}$$

$$f_{\text{hisand}} = 1 - \frac{0.7.\left(1 - \frac{m_s}{100} \right)}{\left(1 - \frac{m_s}{100} \right) + \text{Exp}\left[5.51 + 22.9\left(1 - \frac{m_s}{100} \right) \right]} \tag{14.6}$$

where f_{csand} is a factor that lowers the K indicator in soils with a high proportion of coarse-sand content and higher for soils with little sand; $f_{\text{cl-si}}$ gives low soil erodibility factors for soils with a high clay-to-silt ratio; f_{orgC} reduces the K values in soils with a high organic carbon content while f_{hisand} reduce the K value of soil classes with high sand contents.

Topographic (LS) Factors

The combined slope length and slope angle (LS-factor) describes the effect of topography on soil erosion. The steeper and the longer the slope, the higher is the rate of erosion due to the greater accumulation of runoff (Wischmeier and Smith 1978; Alexakis et al. 2013). In RUSLE, Slope length is defined as the horizontal distance from the origin of overland flow to the point where deposition begins or where runoff flows into a defined channel (Renard et al. 1997; Yahya et al. 2013). However, in a real two-dimensional landscape, overland flow and the resulting soil loss do not depend on the distance, rather on the area per unit of contour length contributing runoff to that point. For this reason, the slope length unit replaced by the unit-contributing area (Desmet and Govers 1996) from digital elevation models (DEMs). Slope length factor (L) is given by the following expression:

$$L = (\lambda/22.13)^m; \ m = \beta/(1 + \beta); \ \beta = \frac{\left(\frac{\text{Sin}\theta}{0.0896} \right)}{(3\left(\text{Sin}\theta^{0.8} \right) + 0.56} \tag{14.7}$$

where λ is the slope length (m), m is the slope length exponent, β is a factor that varies with slope gradient and θ is slope angle. Replacing slope length with unit-contributing areas, the slope length factor $L_{i,j}$ (Desmet and Govers 1996) written as:

$$L_{i,j} = \frac{\left(A_{i,j} + D^2 \right)^{m+1} - A_{i,j}^{m+1}}{D^{m+2}.\ X_{i,j}^m.\ 2.13^m} \tag{14.8}$$

where $A_{i,j}$ is unit-contributing area at the inlet of grid cell, D is grid cell size which is 30 m in this case and $X_{i,j} = \sin \alpha_{i,j} + \cos \alpha_{i,j}$, the $\alpha_{i,j}$ is the aspect direction of the grid cell (i, j).

To obtain a better representation of the Slope Steepness factor, calculation of the S-factor proposed by Wischmeier and Smith (1978)was modified in RUSLE considering ratio of the rill and inter-rill erosion.

$$\begin{cases} S = 10.8 \sin + 0.03, \ \tan < 0.09 \\ 16.8 \sin - 0.50, \ \tan \geq 0.09 \end{cases} \tag{14.9}$$

For calculating the LS factor, LS-TOOL proposed by Zhang et al. (2017) was used in this study.

Cover (C) Factor

The cover and management factor (C) reflects the effect of cropping and management practices on soil erosion rates (Renard et al. 1997). The C-factor is defined as the ratio of soil loss from land with specific vegetation to the corresponding soil loss from continuous fallow (Wischmeier and Smith 1978).

In this study, the C factor was derived from Landsat OLI imagery using Linear Spectral Mixture Analysis (LSMA) approach (De Asis et al. 2008). LSMA has been frequently used to derive subpixel information from remotely sensed imagery (Adams et al. 1995; Lu et al. 2003; He et al. 2010). The basic premise of mixture modeling is that within a given scene, the surface is dominated by a small number of distinct materials called endmembers. The fractions in which the endmembers appear in a mixed pixel are called fractional abundances (Adams et al. 1995; Asis et al. 2008). The selection of endmembers is a critical component for successful application of mixture modeling. The minimum noise fraction (MNF) transformation was applied to the reflectance image to improve quality of fraction images through decorrelation. The result of MNF transformation is then used to calculate the pixel purity index (PPI) to determine the most spectrally pure pixels (endmembers). N-Dimensional Visualizer tool in ENVI software then applied to select the endmembers (He et al. 2010). In reality, three or four endmembers (e.g., green vegetation (GV), shade, soil, and non-photosynthetic vegetation (NPV)) can be used to characterize the variance in the image for LSMA (Asis et al. 2008). Mathematically LSMA model can be expressed as:

$$R_i = \sum f_j r_{ij} + \varepsilon_i; \qquad \sum f_j = 1; \qquad 0 < f_j < 1 \tag{14.10}$$

where R_i is the spectral reflectance of the mixed pixel in band i, f_j is the fraction of the pixel area covered by the endmember j, r_{ij} denotes the reflectance of the endmember j in band i, and ε_i is the root mean square (RMS) in band i.

Table 14.2 Conservation practice (*P*) factor values

Land cover type	Slope (%)	*P* factor
Agriculture land	0–5	0.1
	5–10	0.12
	10–20	0.14
	20–30	0.19
	30–50	0.25
	50–100	0.33
Other land	All	1.00

In this study, the fractional abundance of bare soil and vegetation to define a bare soil to vegetation cover ratio was used as an indicator of susceptibility to soil erosion as follows:

$$C = \frac{F_{bs}}{1 + F_{veg}} \qquad (14.11)$$

where, *C* is RUSLE *C*-factor, F_{bs} and F_{veg} are the fractions of bare soil and vegetation respectively. The equation assumes that soil erosion occurs only when there are exposed soils that are subject to soil detachment by raindrop impact and surface runoff. The addition of 1 in the denominator limits the *C* value between 0 and 1.

Conservation Practice (*P*) Factor

Specific cultivation practices affect erosion by modifying the flow pattern and direction of runoff and by reducing the amount of runoff (Renard et al. 1997). The Conservation practice (*P*) factor is the ratio of soil loss with a specific support practice to the corresponding loss with up slope and down slope cultivation (Wischmeier and Smith 1978). Since there is no complete data on the conservation structures and most of the structures in the study area are not functional due to lack of regular maintenance, the *P*-factor for this study was determined using slope and land cover (Wischmeier and Smith 1978) as shown in Table 14.2.

14.2.3.3 Potential Locations for Ephemeral Gully Formation

To predict the susceptibility of a particular field to ephemeral gully formation, a threshold concept has been adopted (Tamene 2005; Daba et al. 2003). Generally, the gully incision is expected to appear when contributing area together with local slope exceeds a given threshold (Poesen et al. 2003). To predict the potential location and spatial patterns of gullies in the study area, the method proposed by Moore et al. (1988) were used (Fig. 14.3). Upslope contributing area or flow accumulation (As)
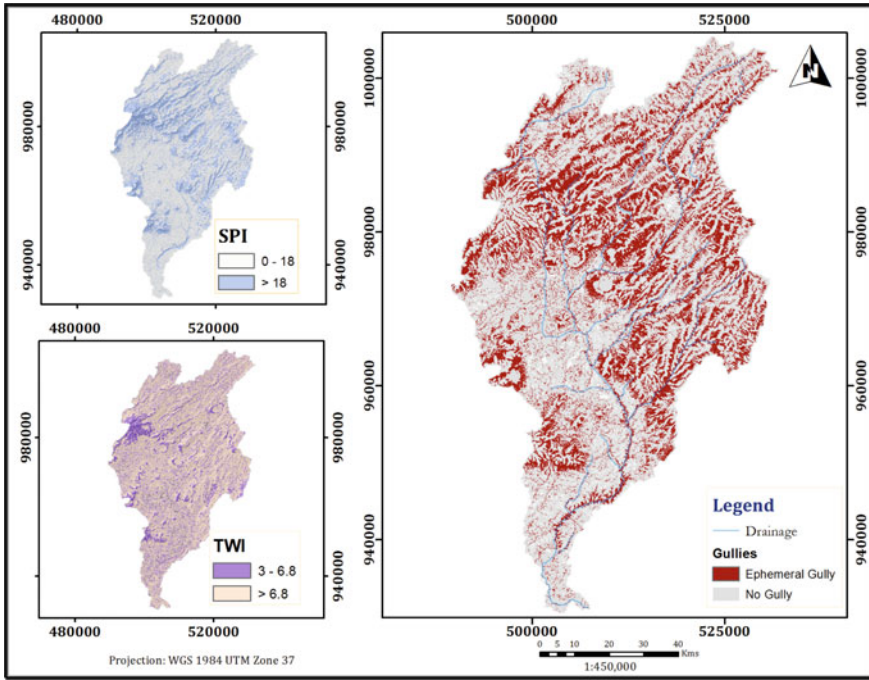
Fig. 14.3 Spatial location of ephemeral gullies

and local slope (β) were generated from DEM of the study area to generate stream power index (SPI) and wetness index (WI) maps using the following equations. Previous studies (Moore et al. 1988; Daba et al. 2003; Tamene 2005) used these indices to predict potential areas of initiation of ephemeral gullies when SPI > 18 and WI > 6.8 (Daba et al. 2003; Tamene 2005).

$$\text{SPI} = \text{As}(\tan \beta) \tag{14.12}$$

$$\text{WI} = \ln(\text{As}/\tan \beta) \tag{14.13}$$

where As = the unit-contributing area (m²/m), β = the local slope (m/m), SPI = stream power index and WI = wetness index.

14.3 Results and Discussion

14.3.1 Potential Soil Loss Based on RUSLE

The various erosion factors (R, K, LS, C and P) for input into the RUSLE and estimate potential annual soil loss for the Mojo River Watershed are presented in Fig. 14.4.

Based on the analysis, the entire watershed loses a total of about 44,992,460.42 tons of soil annually from 1680.41 km^2 of land. Poor vegetation cover is exposing the area to high rates of erosion. As shown in Fig. 14.5, estimated annual soil loss was classified into six erosion severity classes (Singh et al. 1992; Gara et al 2011). MW-wise average soil loss ranges from 2.36 to 47.99 t/ha/year with a mean annual soil loss of 25.83 t/ha/year and standard deviation 12.04.

Table 14.3 shows estimated area of the study area based on annual soil loss in relation to the prevailing slope steepness. A large portion of the study area is classified as slight erosion and it is more than 62% (1045.6 Km^2). This is due to the low average surface slope with plain topography. From the total area, 128.8 Km^2 (7.7%) and 137.4 km^2 (8.2%) reported severe (40–80 t/ha/year) and very severe (>80 t/ha/year) annual erosion rates respectively in all slope classes. Of which, 58.4 Km^2 (3.47%)
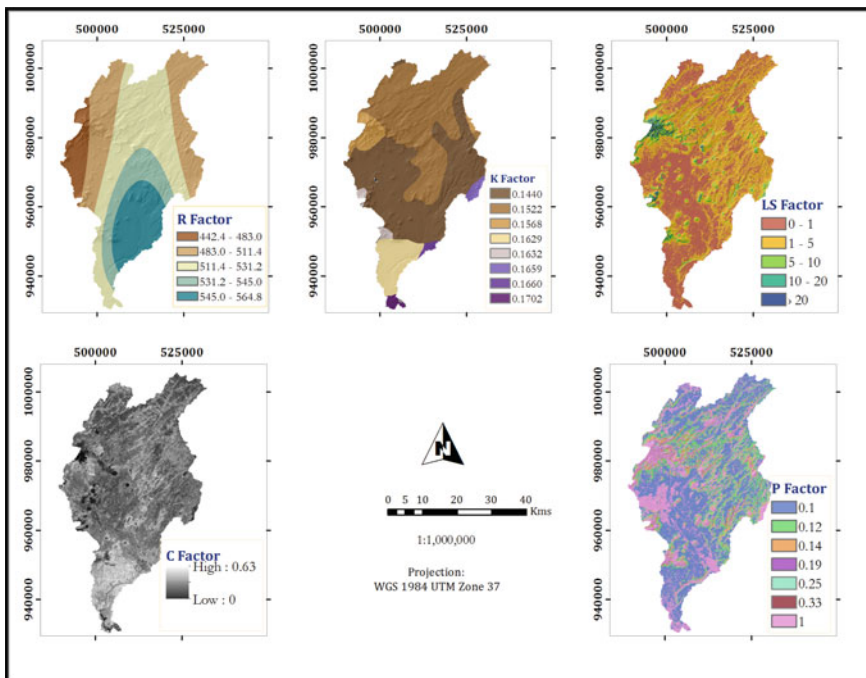

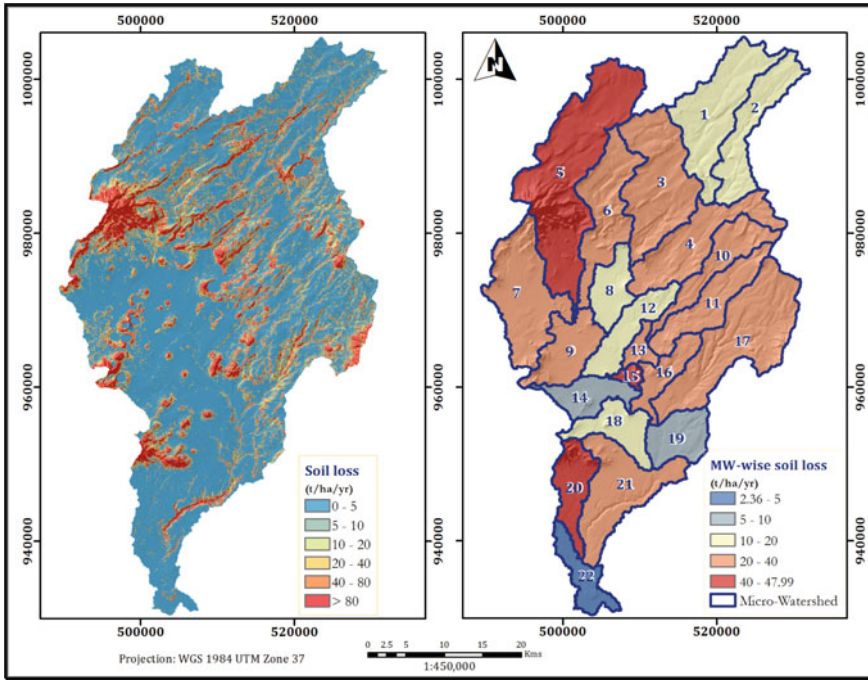**Fig. 14.4** RUSLE factors (R, K, *LS*, C and P) Map

Fig. 14.5 Soil loss map of the study area

within 15–30% slope gradient (moderately steep surface) is under a very severe soil loss class.

14.3.1.1 Prioritization of Micro-watersheds Based on Potential Soil Loss

Prioritization of Micro-watersheds (MWs) has been done on the basis of mean annual soil loss. The result showed that out of the 22 micro-watersheds in Mojo River Watershed, three (MW-5, MW-15 and MW-20) and eleven of them (MW-3, MW-4, MW-6, MW-7, MW-9, MW-10, MW-11, MW-13, MW-16, MW-17, and MW-21) fell under severe (40–47.99 t/ha/year) and very high (20–40 t/ha/year) erosion classes respectively (Table 14.2). These severe and very high erosion rate is due to high contribution from *LS* factor. Severe soil loss is observed in the valley as well as in the ridges of the Mojo River Watershed.

On the basis of annual soil losses, fourteen micro-watersheds that fell under very high and severe erosion classes were found to be critical. These critical MWs with annual mean soil loss greater than 20 t/ha/year were given top and first priority for conservation. As a result, the critical MWs were recommended to adopt the management measures to reduce the soil and nutrient losses.

Table 14.3 Tabulated area (Km²) of soil loss within existing slope gradients

Soil loss class

Slope class description*	Slope (%)	Slight	Moderate	High	Very high	Severe	Very severe	Total area (Km²)	Percent
Flat to very gently sloping	0–2	386.5	0.0	0.0	0.0	0.0	0.0	386.5	23.0
Gently sloping	2–5	552.8	2.7	0.8	45.3	7.5	0.0	609.1	36.2
Sloping	5–10	106.0	167.7	13.6	43.7	78.0	6.7	415.7	24.7
Strongly sloping	10–15	0.2	24.7	31.3	11.7	23.9	36.0	127.7	7.6
Moderately steep	15–30	0.2	0.5	9.2	16.9	17.9	**58.4**	103.1	6.1
Steep	30–60	0.0	0.0	0.0	0.5	1.5	33.1	35.1	2.1
Very steep	>60	0.0	0.0	0.0	0.0	0.0	3.2	3.2	0.2
Area (Km²)		1045.6	195.6	54.8	118.1	**128.8**	**137.4**	1680.4	100.0
Percent		62.2	11.6	3.3	7.0	**7.7**	**8.2**	100.0	

* Modified from FAO (2006)

Previous studies conducted on soil erosion assessment in Ethiopia shows different rate of soil erosion. For example, studies conducted by FAO (1986), in the Ethiopian high lands shows 100 t/ha/year soil loss from cropped lands taking into consideration the redeposit. Another survey conducted on soil and water resources of Ethiopia revealed that the annual soil loss rate ranges from 16 to 300 t/ha/year (Hawando 1995) and 18 to 214.8 t/ha/year (SCRP 1996). According to the Ministry of Water Resource (MoWR 2008), estimates for soil erosion based on the sediment curve at Mojo gauging station and on an average sedimentation rating in Koka reservoir are 15–25 t/ha/year. This has resulted in a loss of 30% of the total storage volume of the reservoir due to siltation (EEPC 2002; Elias 2003).

Removal of vegetation cover due to LULC change and lack of adequate soil and water conservation has largely contributed to increased rates of soil erosion and loss of soil nutrients and top soil (Tegene 2002; Desalegn et al. 2014; Kindu et al. 2018). The implications of soil erosion extend beyond the removal of valuable topsoil. It causes a decline in crop yields. National level estimates reveal a 2% average annual reduction of the agricultural GDP due to erosion (FAO 1986).

14.3.2   Erosion Risk in the Watershed Based on MCE

14.3.2.1   Composite Erosion Index (CEI)

The weight and rating system used for soil erosion intensity map is based on the relative importance of various causative factors (Deore 2005). Four selected criteria layers (slope, NDVI, soil type and gully) were used in multi-criteria analysis to generate Composite Erosion Index (CEI) by Weighted Linear Combination (WLC) as follows:

$$CEI = (W_1 \times Slope) + (W_2 \times NDVI) + (W_3 \times Soil) + (W_{14} \times Gully) \quad (14.14)$$

where CEI is Composite Erosion Index; W_1, W_2, W_3 and W_4 are pairwise weights for reclassified layers of slope, NDVI, soil type, and gully respectively.

Values of CEI in the study area ranges between 1 and 4.41 (dimensionless). Minimal and low erosion potential was present under dense vegetation when the slope gradient was also low but increased with higher slope values. There were few cells with extreme erosion potential, and these were usually restricted along stream channels and ridges with very high slope values. Table 14.4 shows area and proportion of the study area categorized in a classified CEI map.

Assessments of gully erosion volumes in Ethiopia are rare. Using photogrammetric techniques, Daba et al. (2003) estimate that between 1966 and 1996, 700,000 tons of soils were lost by gully erosion from a 9-km^2 watershed in the eastern highlands (26 t/ha/year). Using monitoring and interview techniques to establish average long-term soil loss rates by gully erosion obtained 5 t/ha/year in Central Tigray

Table 14.4 Classification of micro-watersheds based on soil loss

Soil erosion class*	Mean soil loss (t/ha/year)	No. of MWs	Area (Km²)	Percentage
Slight	0–5	1	36.35	2.16
Moderate	5–10	2	89.56	5.33
High	10–20	5	339.17	20.18
Very high	20–40	11	940.89	55.99
Severe	40–47.99	3	274.44	16.33

* Adapted from Singh et al. (1992) and Gara et al. (2011)

(Nyssen 2001). To reduce further expansion of gullies, buffer plantation along gully sides in the study area is required.

14.3.2.2 Prioritization of Micro-watersheds Based on CEI

The intensity of soil erosion indicated by Composite Erosion Index in the MWs is considered for their prioritization for selection and implementation of conservation measures and plan appropriate land use to minimize the soil losses in them (Tripathi et al. 2003; Deore 2005; Khan et al. 2001). All 22 micro-watershed were grouped into five CEI classes (Fig. 14.6) based on the data natural breaks. Micro-watershed wise mean CEI indicates that MW-3, MW-4, MW-6, and MW-12 are under very high CEI category with a value above 2.16. The area covered under this category is 389.77 Km² (23.2%). High CEI category is represented by six MWs covering 622.85 Km² area (37.07%). Most parts of these micro-watersheds are under low vegetation cover and high proportion of ephemeral gullies which causing high erosion intensity. CEI class in Table 14.5 was just based on Natural breaks (Jenks) classification mehtod used in ArcGIS symbology.

14.4 Conclusions

Application of RUSLE model and MCE in GIS environment can help watershed managers in assessing and identifying erosion prone areas for undertaking required conservation measures. The landscape positions where steep slope, poor surface cover, erodible soil, and gully erosion coincided show high erosion risk compared to others. Based on the RUSLE model, MW-wise average annual soil loss ranges from 2.36 to 47.99 t/ha/year with a mean annual soil loss of 25.83 t/ha/year and standard deviation 12.04. Based on MCE approach, micro-watershed wise mean CEI ranges from 1.71 to 2.31 with a mean value of 2.06. Four micro-watersheds (MW-3, MW-4, MW-6, and MW-12) are under very high CEI category covering 389.77 Km² (23.2%) with a value above 2.16. Most parts of these micro-watersheds are under cultivated
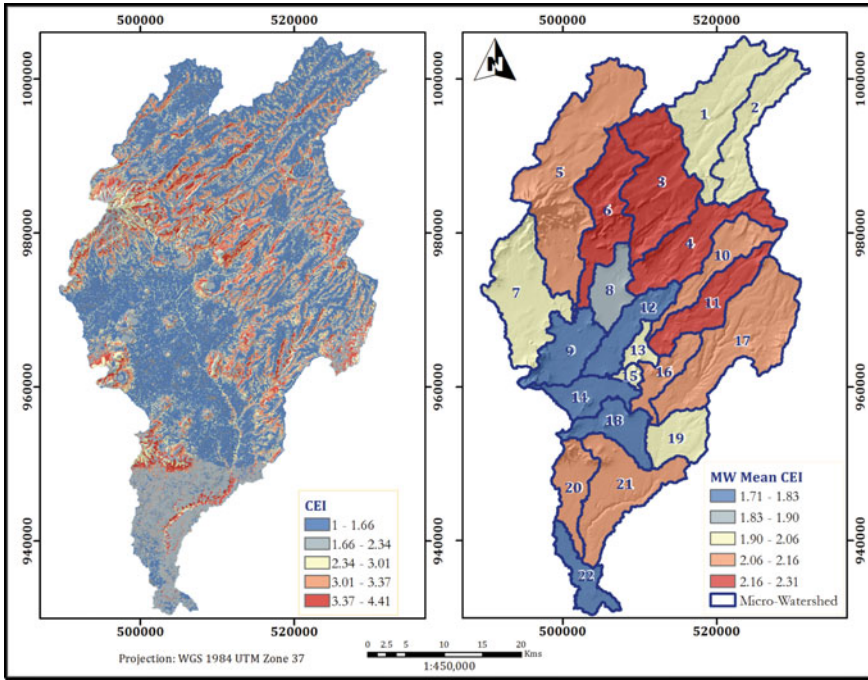
Fig. 14.6 Micro-watershed wise Composite Erosion Index map

Table 14.5 Categorization and prioritization of Micro-watersheds based on CEI

CEI class	Mean CEI	No. of MWs	Area (Km^2)	Percentage
Very low	1.71–1.83	5	239.89	14.28
Low	1.83–1.90	1	42.49	2.53
Moderate	1.90–2.06	6	385.41	22.94
High	2.06–2.16	6	622.85	37.07
Very high	2.16–2.31	4	389.77	23.20

and bare land and high proportion of ephemeral gullies which causing high erosion intensity.

Based on the result, the micro-watersheds which fall under very high and high categories need immediate attention in their order of soil erosion potential. Therefore, for reducing further degradation, reclaiming the degraded areas and improving the land productivity of the watershed, and reducing their sediment delivery to low lands and reservoirs, hot-spot areas having a large rate of erosion should be given first priority for well-designed conservation interventions in the study area.

References

Adams JB, Sabol DE, Kapos V, Filho RA, Roberts DA, Smith MO, Gillespie A (1995) Classification of multispectral images based on fractions of endmembers: application to land-cover change in the the Brazilian Amazon. Remote Sens Environ 52(2):137–154

Adimassu Z, Mekonnen K, Yirga C, Kessler A (2014) Effect of soil bunds on runoff, soil and nutrient losses, and crop yield in the central highlands of Ethiopia. Land Degrad Dev 25:554–564

Alexakis D, Hadjimitsis D, Agapiou A (2013) Integrated use of remote sensing, GIS and precipitation data for the assessment of soil erosion rate in the catchment area of "Yialias" in Cyprus. Atmos Res 131:108–124

Bewket W (2002) Land cover dynamics since the 1950s in Chemoga Watershed, Blue Nile Basin, Ethiopia. Mt Res Dev 22:263–269

Central Statistical Agency (CSA) (2007). Population and housing census of Ethiopia. Addis Ababa, Ethiopia

Daba S, Rieger W, Strauss P (2003) Assessment of gully erosion in eastern Ethiopia using photogrammetric techniques. Catena 50:273–291

De Asis AM, Omasa K, Oki K, Shimizu Y (2008) Accuracy and applicability of linear spectral unmixing in delineating potential erosion areas in tropical watersheds. Int J Remote Sens 29(14):4151–4171

Daba S, Rieger W, & Strauss P (2003) Assessment of gully erosion in eastern Ethiopia using photogrammetric techniques. CATENA 50(2-4):273–291

Demissie F, Yeshitila K, Kindu M, Schneider T (2017) Land use/land cover changes and their causes in Libokemkem District of South Gonder, Ethiopia. Remote Sens Appl Soc Environ 8:224–230

Deore SJ (2005) Prioritization of Micro-watersheds of Upper Bhama Basin on the basis of soil erosion risk using remote sensing and GIS technology. PhD thesis, University of Pune, Pune

Desalegn T, Cruz F, Kindu M, Turrión M, Gonzalo J (2014) Land-use/land-cover (LULC) change and socioeconomic conditions of local community in the central highlands of Ethiopia. Int J Sust Dev World 21(5):406–413

Desmet PJJ, Govers, G. (1996) A GIS procedure for automatically calculating the USLE LS factor on topographically complex landscape units. J Soil Water Conserv 51(5):427–433

EEPC (2002) Koka Dam sedimentation study: recommendations report. Ethiopian electric power corporation. Addis Ababa, June 2002

Elias E (2003) Case studies: genetic diversity, coffee and soil erosion in Ethiopia. Roles of agriculture project international conference, Rome, Italy, 20–22 Oct 2003

Ethiopian Roads Authority (2007) Ethiopian road map. Non-authoritative border. Data from 1984-2005. Addis Ababa, Ethiopia

FAO (1986) Ethiopia Highlands Reclamation Study. Final Report, vol 1. FAO, Rome

FAO (2019) Soil erosion: the greatest challenge to sustainable soil management. Licence: CC BY-NC-SA 3.0 IGO, Rome, p 100

Gara A, Suzuki S, Watanabe F, Himadas S, Toyoda H (2011) Soil erosion assessment using USLE in East Shewa, Ethiopia. J. Agric. Sci. Tokyo Univ. Agric. 56(1), 1–8

Gashaw T, Taffa T, Argaw M, Worqlul AW, Tolessa T, Kindu M (2018) Estimating the impacts of land use/land cover changes on ecosystem service values: the case of the Andassa watershed in the Upper Blue Nile basin of Ethiopia. Ecosyst Serv 31:219–228

Haregeweyn N, Tsunekawa A, Nyssen J, Tsubo M, Meshesha DT, Schutt B, Adgo E, Tegegne F (2015) Soil erosion and conservation in Ethiopia: a review. Prog Phys Geogr 39(6):750–774

Hawando T (1995) The survey of the soil and water resources of Ethiopia. NU/Toko

He M, Zhao B, Ouyang Z, Yan Y, Li B (2010) Linear spectral mixture analysis of Landsat TM data for monitoring invasive exotic plants in estuarine wetlands. Int J Remote Sens 31(16):4319–4333

Hellden U (1987) An assessment of woody biomass, community forests, land use and soil erosion in Ethiopia. Lund University Press

Hurni H (1985) Soil conservation manual for Ethiopia. First draft. Ministry of Agriculture, Natural Resources Conservation and Development Department, Community Forests and Soil Conservation Development Department, Addis Ababa

Hurni H (1993) Land Degradation, famine and resource scenarios in Ethiopia. In: Pimentel D (ed) World soil erosion and conservation, Cambridge University press, Cambridge

Khan MA, Gupta VP, Moharana PC (2001) Watershed prioritization using remote sensing and geographical information system: a case study from Guhiya, India. J Arid Environ 49:465–475

Kindu M, Schneider T, Teketay D, Knoke T (2013) Land use/land cover change analysis using object-based classification approach in Munessa-Shashemene landscape of the Ethiopian highlands. Remote Sens 5(5):2411–2435

Kindu M, Schneider T, Teketay D, Knoke T (2015) Drivers of land use/land cover changes in munessa-shashemene landscape of the south-central highlands of Ethiopia. Environmental Monitoring and Assessment 187(7):452

Kindu M, Schneider T, Teketay D, Knoke T (2016) Changes of ecosystem service values in response to land use/land cover dynamics in Munessa-Shashemene Landscape of the Ethiopian highlands. Sci Total Environ 547:137–147

Kindu M, Schneider T, Döllerer M, Teketay D, Knoke T (2018) Scenario modelling of land use/land cover changes in Munessa-Shashemene landscape of the Ethiopian highlands. Sci Total Environ 622–623:534–546

Lu D, Moran E, Batistella M (2003) Linear mixture model applied to Amazonian vegetation classification. Remote Sens Environ 87:456–469

Ministry of Water Resources (MoWR) (1999) Survey of the awash river basin. Vol II. Soils and agronomy. Integrated Development Master Plan Study. Addis Ababa, Ethiopia

Moore ID, Burch GJ, Mackenzie DH (1988) Topographic effects on the distribution of surface soil water and the location of ephemeral gullies. Trans ASAE 31(4):1098–1107

MoWR (2008) Awash River basin flood control and watershed management project. Feasibility report for Mojo River badlands rehabilitation. Main report

Nyssen J (2001) Erosion processes and soil conservation in a tropical mountain catchment under threat of anthropogenic desertification – a case study from Northern Ethiopia. PhD thesis, Department of Geography, K.U. Leuven, Belgium

Poesen J, Nachtergaele J, Verstraeten G, Valentin C (2003) Gully erosion and environmental change: importance and research needs. Catena 50:91–133

Renard KG, Foster GR, Weesies GA, McCool DK, Yoder DC (1997) Predicting soil erosion by water: a guide to conservation planning with the revised universal soil loss equation (RUSLE). US Department of Agriculture, Agricultural Handbook Number, vol. 703. Government Printing Office, Washington

SCRP (1996) Soil erosion hazard assessment for land evaluation. University of Bern, Switzerland, in association with Ministry of Agriculture, Government of Ethiopia

Shi ZH, Cai CF, Ding SW, Wang TW, Chow TL (2003) Soil conservation planning at the small watershed level using RUSLE with GIS: a case study in the Three Gorge Area of China. Catena 55:33–48

Singh G, Babu R, Narayan P (1992) Soil erosion rates in India. J Soil Water Conserv 47:97–99

Sutcliff, J.P. (1993). Economic assessment of land degradation in the Ethiopian highlands: a case study. National conservation strategy secretariat, Ministry of planning and economic development, Addis Ababa, Ethiopia

Tamene, L. (2005). Reservoir siltation in Ethiopia: causes, source areas, and management options. Ecology and Development Series No. 30. Center for Development Research, Bonn, Germany

Tamene L, Vlek PLG (2007) Assessing the potential of changing land use for reducing soil erosion and sediment yield of catchments: a case study in the highlands of northern Ethiopia. Soil Use Manag 23:82–91

Tegene B (2002) Land-cover/land-use changes in the derekolli catchment of the South Welo Zone of Amhara Region, Ethiopia. East Afr Soc Sci Res Rev 18:1–20

Temesgen H, Nyssen J, Zenebe A, Haregewey N, Kindu M, Lemenih M, Haile M (2013) Ecological succession and land use changes in a lake retreat area (Main Ethiopian Rift Valley). J Arid Environ 91, 53–60

Tripathi MP, Panda RK, Raghuwanshi NS (2003) Identification and prioritization of critical sub-watersheds for soil conservation management using the SWAT model. Biosys Eng 85(3):365–379

Wischmeier WH, Smith DD (1978) Predicting rainfall erosion losses: a guide to conservation planning. In: Agriculture handbook No. 537. US Department of Agriculture, Washington DC

Yahya F, Zregat D, Farhan I (2013) Spatial estimation of soil erosion risk using RUSLE approach, RS, and GIS techniques: a case study of Kufranja Watershed Northern Jordan. J Water Res Prot 5:1247–1261

Zhang H, Wei J, Yang Q, Baartman JEM, Gai L, Xiaomei Yang X, Li S, Yu J, Ritsema CJ, Geissen V (2017) An improved method for calculating slope length (λ) and the LS parameters of the revised universal soil loss equation for large watersheds. Geoderma 308(2017):36–45